Liquid Crystals
Publication details, including instructions for authors and subscription information:
http://www.informaworld.com/smpp/title~content=t713926090

Fabrication and characterization of polymer stabilized cholesteric liquid crystal cells with chiral monomers derived from borneol

Jui-Hsiang Liu[a]; Hsien-Jung Hung[b]
[a] Department of Chemical Engineering and Institute of Electro-optics, National Cheng Kung University, Tainan, Taiwan 70101, ROC [b] Department of Chemical Engineering, National Cheng Kung University, Tainan, Taiwan 70101, ROC

To cite this Article Liu, Jui-Hsiang and Hung, Hsien-Jung(2005) 'Fabrication and characterization of polymer stabilized cholesteric liquid crystal cells with chiral monomers derived from borneol', Liquid Crystals, 32: 1, 133 — 142
To link to this Article: DOI: 10.1080/02678290412331329260
URL: http://dx.doi.org/10.1080/02678290412331329260

Liquid Crystals, Vol. 32, No. 1, January 2005, 133–142

Taylor & Francis
Taylor & Francis Group

Fabrication and characterization of polymer stabilized cholesteric liquid crystal cells with chiral monomers derived from borneol

JUI-HSIANG LIU*† and HSIEN-JUNG HUNG‡

†Department of Chemical Engineering and Institute of Electro-optics, National Cheng Kung University, Tainan, Taiwan 70101, ROC

‡Department of Chemical Engineering, National Cheng Kung University, Tainan, Taiwan 70101, ROC

(*Received 20 June 2004; accepted 25 September 2004*)

Polymer stabilized cholesteric texture (PSCT) liquid crystal cells were fabricated using the commercially available host liquid crystal ZLI-2293/CB15 and functional monomers 4,4′-bis[6-(acryloyxy)hexyloxy]biphenyl (BAHB) and bornyl 4-[4-(6-acryloyloxyhexyloxy)phenylazo] benzoate. Monomers synthesized in this investigation were identified using FTIR, ^{1}H NMR and elemental analysis. Optical properties of the PSCT cells were studied, including variations in the reflected band, the pitch, and the helical twisting power. The dependence of the variation of liquid crystal texture on UV irradiation, temperature, and voltage were estimated. A schematic molecular orientation of the cells was used to describe the phenomena obtained on application of a voltage. Due to the thick film gap, surface stabilization from the polymer matrixes on the substrates was found to be unable to fix the focal-conic texture, even when the cell was slowly released from the applied field. The liquid crystal molecules returned to a planar texture in few seconds. The real images of reflected band colours, and the reversible changes between the turbid and transparent states corresponding to OFF (30 V) and ON (100 V) applied electric fields were evaluated.

1. Introduction

Liquid crystal polymer dispersions have considerable potential for large area displays and light control applications, since they can be switched electrically from a light-scattering to a transparent state and do not require polarizers and alignment layers [1–4]. The dispersion of a small amount of polymer in a liquid crystal matrix (polymer stabilized liquid crystal) has shown considerable promise for liquid crystal display applications [5–7]. These polymers have high surface areas and consequently tend to stabilize liquid crystal order efficiently, even at low concentration.

Some reflective colour displays use scattering liquid crystal materials, such as polymer dispersed liquid crystal (PDLC) materials or scattering-mode polymer stabilized cholesteric texture materials, to control the intensity of light reflected from each pixel by switching between a turbid state and a uniform state [8–10]. Since these materials scatter light only weakly in their turbid state, reflective displays based on them have a low diffuse reflectance and therefore also suffer from low brightness [11]. Other reflective colour displays use reflecting liquid crystal materials, such as reflective-mode polymer stabilized cholesteric texture (PSCT) materials or holographic polymer dispersed liquid crystals, to control both the intensity and colour of light reflected from each pixel via diffraction effects [12–14]. It is difficult simultaneously to achieve a large viewing angle, high reflectance, and angle independent colour [15].

The reflective nature of reflective liquid crystal displays (LCDs) can reduce power consumption by one-half by eliminating backlight requirements [16]. Further reduction in power consumption in reflective LCDs can be achieved in PSCT liquid crystal displays [17–20]. These possess a cholesteric liquid crystal medium containing a stabilizing polymer network. We have previously prepared PDLC membranes and studied their optical properties and matrix morphologies [21–23].

In this study, we synthesized chiral and difunctional monomers and fabricated polymer stabilized cholesteric liquid crystals. The reflected light wavelength [24], optical textures, and pitches of the cholesteric liquid crystal cells were investigated. The dependence of reflected wavelength on temperature, UV irradiation, and applied voltage were studied. Real image recording and reversible changes between the turbid and transparent states corresponding to the fields were also confirmed.

*Corresponding author. Email: jhliu@mail.ncku.edu.tw

Liquid Crystals
ISSN 0267-8292 print/ISSN 1366-5855 online
http://www.tandf.co.uk/journals
DOI: 10.1080/02678290412331329260

2. Experimental

2.1. *Characterization*

FTIR spectra were recorded on a Jasco VALOR III Fourier transform infrared spectrophotometer. Nuclear magnetic resonance (NMR) spectra were obtained on a Bruker AMX-400 high resolution NMR spectrometer. Optical rotations were measured at 30°C in dimethylformamide (DMF) using a Jasco DIP-360 automatic digital polarimeter with readings to $\pm 0.001°$. Elemental analyses were conducted with a Heraeus CHN-O rapid elemental analyser. Gel permeation chromatography (GPC) measurements were carried out at 40°C on a Hitachi L-4200 instrument equipped with TSK gel GMH and G2000H columns using THF as an eluent.

Thermal analysis of the azobenzene compounds and PDLC films was performed by differential scanning calorimetry (DSC, Perkin-Elmer) at a heating and cooling rate of $10\,K\,min^{-1}$ in a nitrogen atmosphere. The liquid crystal phases were investigated by polarizing optical microscopy (POM, Olympus BH-2), using a Mettler hot stage (Model FP-82) and temperature scanning rate of $5\,K\,min^{-1}$.

2.2. *Synthesis*

The difunctional 4,4′-bis[6-(acryloyxy)hexyloxy]biphenyl (BAHB) was synthesized according to a reported method [25]. Synthetic routes for the chiral monomer are shown in scheme 1. The chiral bornyl derived monomers were synthesized by similar literature procedures [26, 27].

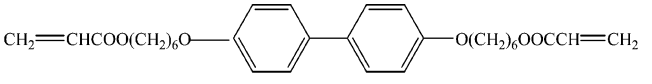

BAHB

2.2.1. 4-Hydroxy-4′-ethoxycarbonylazobenzol (1). Ethyl 4-aminobenzoate (10 g, 60.6 mmol) was dissolved in 1M aqueous HCl (100 ml) and held in an ice bath at 0°C. $NaNO_2$ (4.2 g, 60.8 mmol) dissolved in water (30 ml) was added dropwise to the solution and the mixture stirred for 30 min. NaOH (7.2 g, 0.18 mol) and phenol (5.8 g, 61.7 mmol) were dissolved in water (80 ml), and stirred for 30 min at 0°C the first solution was then added dropwise, the temperature held at 0°C and stirring main tained for 1 h. The resulting mixture was poured into water and the solution neutralized with 5% aqueous HCl. The crude product was filtered off and recrystallized twice from EtOH; yield 11.8 g (72%) of a red crystalline powder, T_m=153–154°C. FTIR (cm^{-1}): 3399 (OH), 2973, 2927, 2906 (–CH_2–), 1693 (C=O in Ar–COO–), 1601, 1504 (C–C in Ar). ^{1}H NMR (acetone-d6, δ ppm): 1.38 (t, 3H, $OCH_2\underline{CH_3}$), 4.35 (q, 2H, $OC\underline{H_2}CH_3$), 7.03–8.17 (m, 8H, aromatic).

2.2.2. Ethyl 4-[4-(6-hydroxyhexyloxy)phenylazo]benzoate (2). KOH (4.3 g, 76.2 mmol) dissolved in EtOH (100 ml) was added dropwise to a solution of compound **1** (18.7 g, 69.3 mmol) in EtOH (100 ml). 1-Cholo-6-hexenol (14.5 g, 103.9 mmol) and KI (3 g, 18.1 mmol) were then added, and the mixture heated at reflux for 30 h. The resulting mixture was poured into water and extracted with CH_2Cl_2. The precipitate was filtered and washed with water. The crude product was recrystallized twice from EtOH; yield 19.5 g (76%), T_c=28–29°C, T_m=90–91°C. FTIR (cm^{-1}): 3557 (OH), 2940, 2864 (CH_2), 1706 (C=O in Ar–COO–), 1600, 1501 (C–C in Ar), 1260 (COC). ^{1}H NMR (acetone-d6, δ ppm): 1.33–1.80 (m, 11H, methyl), 3.43 (t, 2H, $HOC\underline{H_2}CH_2$), 4.13 (t, 2H, $OC\underline{H_2}CH_2$), 4.39 (q, 2H, $OC\underline{H_2}CH_3$), 7.04–8.18 (m, 8H, aromatic).

2.2.3. Ethyl 4-{4-[6-(tetrahydro-2-pyranyl)hexyloxy]-phenylazo}benzoate (3). Compound **2** (18.0 g, 48.6 mmol) was dissolved in CH_2Cl_2 (100 ml) with a catalytic amount of *p*-toluenesulphonic acid (*p*-TSA) at 35°C. 3,4-Dihydro-2H-pyran (16.4 g, 194.4 mmol) was added dropwise and the mixture stirred for 24 h. The reaction mixture was washed with 5% aqueous $NaHCO_3$ and water; it was dried over Na_2SO_4, and the solvent evaporated. The product was purified by column chromatography (silica gel, ethyl acetate/hexane, 1/8) and recrystallized twice from EtOH; yield 18.7 g (85%), T_c=23–24°C, T_m=48–49°C. FTIR (cm^{-1}): 2948, 2860 (CH_2), 1725 (C=O in Ar–COO–), 1601, 1498 (C–C in Ar), 1272, 1247 (COC). ^{1}H NMR ($CDCl_3$, δ ppm): 1.40–1.84 (m, 17H, methyl), 3.40–3.51 (m, 2H, $OC\underline{H_2}CH_2$), 3.75–3.87 (m, 2H, $OC\underline{H_2}CH_2$), 4.05 (m, 2H, $OC\underline{H_2}CH_2$), 4.41 (q, 2H, $OC\underline{H_2}CH_3$), 4.58 (m, 1H, $OC\underline{H}CH_2O$), 7.01–8.17 (m, 8H, aromatic).

2.2.4. 4-{4-[6-(Tetrahydro-2-pyranyl)hexyoxy]phenylazo}-benzoic acid (4). Compound **3** (18.0 g, 39.6 mmol) was dissolved in CH_2Cl_2 (50 ml). KOH (8.8 g, 158.4 mmol) dissolved in EtOH/water (5/1, 100 ml) was then added and the solution heated at reflux for 24 h. The solvent was then removed from the reaction mixture under vacuum. The resulting suspension was poured into water and the mixture neutralized with dilute HCl to pH=5. The resulting precipitate was filtered,

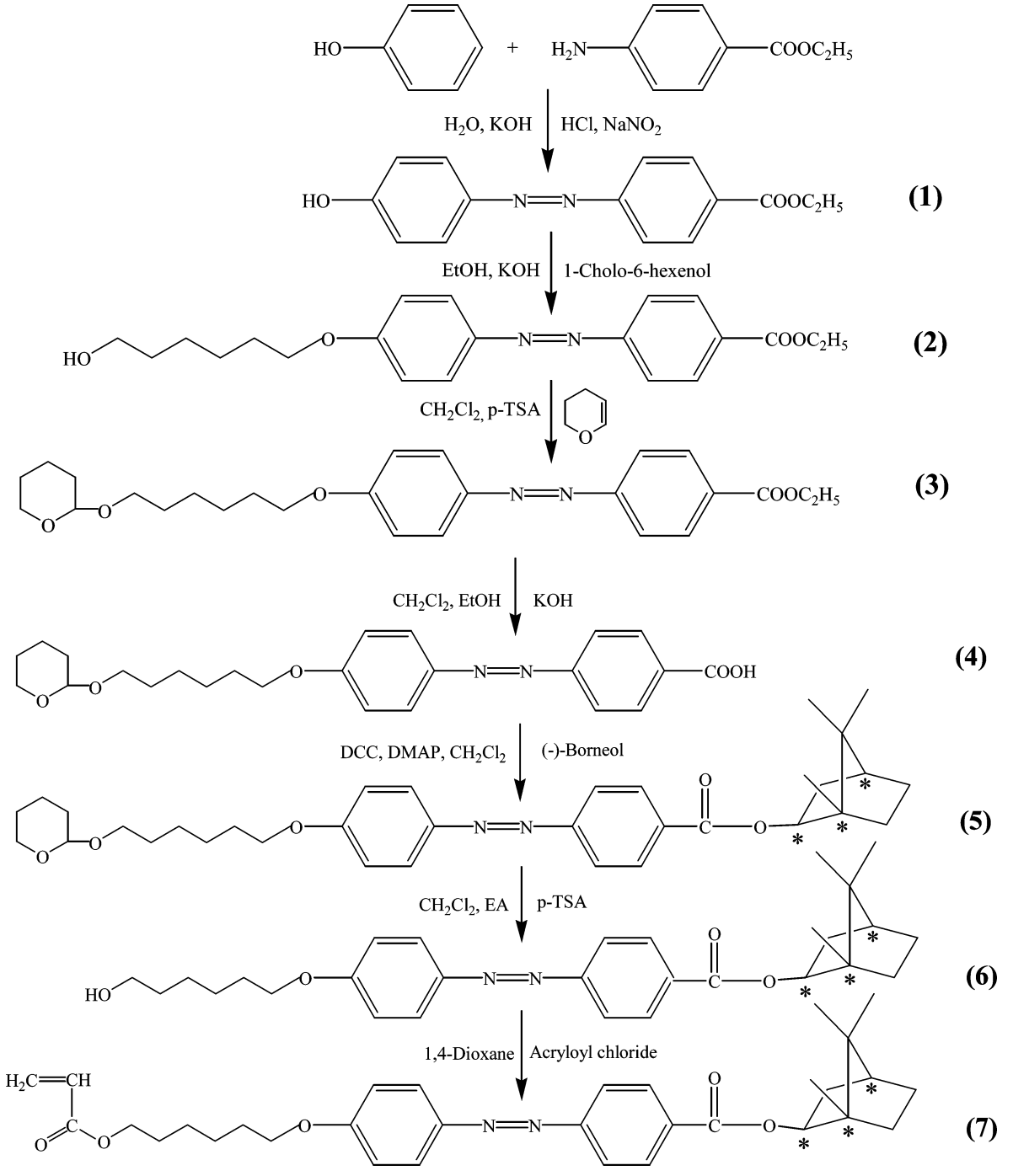

Scheme 1.

washed five times with water, then recrystallized twice from EtOH; yield 15.2 g (90%), T_m=171–172°C. FTIR (cm^{-1}): 2941, 2866 (CH_2), 1682 (C=O in Ar–COO–), 1603, 1497 (C–C in Ar), 1278, 1251 (COC), 2659, 2545 (COOH). ^{1}H NMR (DMSO-d6, δ ppm): 1.42–1.75 (m, 14H, methyl), 3.41 (m, 2H, OC$\underline{H_2}$CH$_2$), 3.68 (m, 2H, OC$\underline{H_2}$CH$_2$), 4.06 (m, 2H, OC$\underline{H_2}$CH$_2$), 4.52 (m, 1H, OC$\underline{H}$CH$_2$O), 6.85–8.11 (m, 8H, aromatic).

2.2.5. Bornyl 4-{4-[6-(tetrahydro-2-pyranyl)hexyloxy]-phenylazo}benzoate (5). Compound **4** (15 g, 35.2 mmol) and (−)-borneol (5.5 g, 35.2 mmol) were dissolved in CH_2Cl_2 (100 ml) at 30°C. *N*,*N*′-dicyclohexylcarbodiimide

(DCC) (29.0 g, 140.8 mmol) and *N*,*N*′-dimethylaminopyridine (DMAP) (0.43 g. 3.52 mmol) were dissolved in CH_2Cl_2 (50 ml), and the solution added to the first solution; the mixture was stirred for 2 days at 30°C. The resulting solution was washed with water, dried over sodium sulphate, and the solvent evaporated. The crude product was purified by column chromatography (silica gel, ethyl acetate/hexane=1/9) and recrystallized twice from EtOH; yield 9.2 g (45%), T_c=26–27°C, T_m=82–83°C. FTIR (cm^{-1}): 2938, 2867 (CH_2), 1705 (C=O in Ar–COO–), 1602, 1499 (C–C in Ar), 1270, 1248 (COC). ^{1}H NMR ($CDCl_3$, δ ppm): 1.13–2.50 (m, 30H, methyl), 3.41 (m, 2H, OC$\underline{H_2}$CH_2), 3.68 (m, 2H, OC$\underline{H_2}$CH_2), 4.06 (m, 2H, OC$\underline{H_2}$CH_2), 4.58 (m, 1H, OC$\underline{H}$CH_2O), 5.13 (m, 1H, COOC$\underline{H}$C), 7.02–8.18 (m, 8H, aromatic).

2.2.6. Bornyl 4-[4-(6-hydroxyhexyloxy)phenylazo]-benzoate (6). Compound **5** (9.0 g, 15.5 mmol) was dissolved in CH_2Cl_2 (50 ml). Ethyl acetate (50 ml), and a catalytic amount of *p*-TSA was then added to the solution, which was stirred for 12 h at 45°C. After completion of the reaction, the solvent was evaporated. The crude product was purified by column chromatography (silica gel, ethyl acetate/hexane=1/9) and recrystallized twice from EtOH; yield 5.9 g (77%), T_c=28–29°C, T_m=91–92°C. FTIR (cm^{-1}): 3329 (OH), 2936, 2864 (CH_2), 1711 (C=O in Ar–COO–), 1604, 1497 (C–C in Ar), 1273, 1251 (COC). ^{1}H NMR ($CDCl_3$, δ ppm): 1.13–2.50 (m, 30H, methyl), 3.68 (m, 2H, OC$\underline{H_2}$CH_2), 4.06 (m, 2H, OC$\underline{H_2}$CH_2), 5.13 (m, 1H, COOC$\underline{H}$C), 7.02–8.18 (m, 8H, aromatic).

2.2.7. Bornyl 4-[4-(6-acryloyloxyhexyloxy)phenylazo]-benzoate (7). Compound **6** (5.5 g, 11.0 mmol), *N*,*N*-dimethylaniline (1.5 g, 12.1 mmol), and a catalytic amount of 2,6-di-*tert*-butyl-*p*-cresol were dissolved in 1,4-dioxane (50 ml). The solution was cooled in an ice/salt bath, then acryloyl chloride (3 ml, 33.1 mmol) dissolved in 1,4-dioxane (20 ml) was added dropwise with vigorous stirring. The mixture was stirred for 24 h at room temperature, then poured into cold water and the precipitate filtered. The crude product was washed with water and recrystallized twice from EtOH; yield 4.7 g (73%), T_m=97–98°C. FTIR (cm^{-1}): 2945, 2864 (CH_2), 1720 (C=O in Ar–COO–), 1600, 1506 (C–C in Ar), 1255, 1282 (COC), 1640 (C=C). ^{1}H NMR ($CDCl_3$, δ ppm): 0.93–2.50 (m, 24H, methyl), 4.06 (m, 2H, OC$\underline{H_2}$CH_2), 4.18 (m, 2H, OC$\underline{H_2}$CH_2), 5.15 (m, 1H, COOC$\underline{H}$C), 5.83(dd, 1H, C$\underline{H_2}$=CH), 6.13(dd, 1H, C$\underline{H_2}$=CH), 6.42(dd, 1H, CH$_2$=C$\underline{H}$), 7.01–8.18 (m, 8H, aromatic). Elemental analysis for $C_{32}H_{40}O_5N_2$ (532): cald, C 72.18, H 7.52, N 5.26; found, C 72.22, H 7.50, N 5.23%.

2.3. *PSCT cell preparation and measurements*

In a reverse mode PSCT, a cholesteric with a pitch of several microns is situated between two plates with homogeneous planar boundary conditions. A low concentration of a reactive monomer is dissolved in the liquid crystal. The monomer is then photopolymerized while the cholesteric is in the planar state; the resulting polymer network should thus reflect the helical structure of the planar state.

The liquid crystal composite cells were prepared from a mixture of ZLI2293/CB15/mono- and difunctional monomers. Since ZLI2293 is a nematic liquid crystal mixture, the composition is complex. For convenience, weight ratios of ZLI2293/CB15/mono- and difunctional monomers were used. The mixture was ultrasonically treated to form a homogeneous solution, then injected into an ITO glass cell separated with a 12 μm spacer. The surfaces of the ITO substrates were pretreated with polyimide and oriented in parallel directions. To prepare PSCT cells, sample cells with the monomer/liquid crystal mixture were cured by UV irradiation of 0.65 mW cm^{-2}. After completing the polymerization, PSCT composite films could be fabricated, assisted by to the surface treatment of the substrates, and the pitch length of the cholesteric liquid crystal.

The optical behaviour of the PSCT cells was investigated using a spectrometer. The optical change of the samples induced by an electric field was monitored by detecting the intensity of the probe light transmitted through the samples with a photodiode. The intensity of the probe light in the absence of the electric field was defined as 100% light transmittance. The optical texture of the composite films was observed under crossed polarizers with a polarizing microscope. Morphological observation of the solid polymer in the composite films was performed with a scanning electron microscope (SEM).

3. Results and discussion

Chiral monomeric bornyl 4-[4-(6-acryloyloxyhexyloxy)-phenylazo] benzoate (**7**) and difunctional 4,4′-bis[6-(acryloyxy)- hexyloxy]biphenyl (BAHB, scheme 2) were synthesized. The synthesized products were identified using ^{1}H NMR, FTIR, and elemental analysis. Polymer stabilized cholesteric liquid crystal cells were fabricated using host ZLI2293/CB15 liquid crystal with various amounts of monomers. The compositions and optical properties of the sample cells are summarized in table 1. The clearing point of the cells decreased with increasing

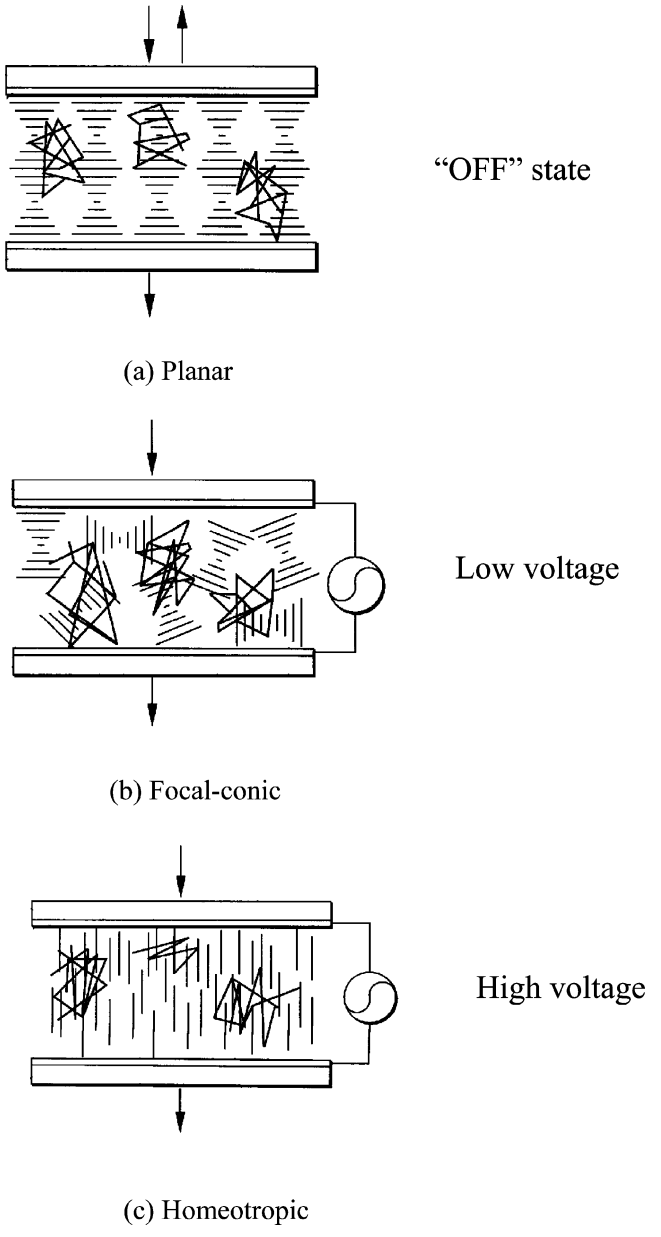

Scheme 2.

of content added chiral monomer **7**, due to disturbance of the orientation order of the host liquid crystal. On reaching the clearing point, the host liquid crystal may completely lose orientation order and change to the isotropic liquid phase.

Figure 1 shows the effect of UV curing on the sample cells. Before curing, cholesteric liquid crystal cells showed standard optical characteristics and reflected a certain band ($\Delta\lambda$) of incident light. As shown in table 1, λ_0 was shifted to the blue side when the concentration of the chiral monomer **7** was increased, indicating that an increase of the chiral component may shorten the helix pitch of the cholesteric liquid crystal cells. After UV curing, as shown in figure 1 (*b*), λ_0 of the cells was shifted to the red side; polymerization of the chiral monomer thus reduced the concentration chiral component in the liquid crystal leading to the red shift of the reflected band. The pitches and helical twisting power (HTP) of the sample cells were evaluated and are summarized in table 1, where it is seen that the shorter the helical pitch the higher the HTP power.

The synthesized chiral monomer **7** is a photo-isomerizable azo derivative. Figure 2 shows the results of UV irradiation with various amounts of **7**. Because cell A_0 contained no azo derivative, UV irradiation did not affect the reflected band, as shown in figure 2 (*a*). For cell A_1, due to the effects of the photo-isomerizable azo component, the reflected band of the sample cell was shifted to the red side. The variation of the absorption band around 370 nm is the result of azo isomerization and decreased with increasing UV irradiation time. As can be seen in figure 2 (*c*), cell A_2 had the same tendency. Red shifts of the reflected bands were obtained, and absorption around the UV area decreased with an increase of the UV irradiation time. The reflected band and the band shifts of the sample cells are summarized in table 2.

An increase of cell temperature may raise the mobility of the liquid crystal molecules and also affect their orientation order. Figure 3 shows the effect of

Table 1. Optical properties of PSCT cells.

		λ_0/nm					
Cell	A6B/mmol[a]	Before[b]	After[c]	$\Delta\lambda_0$	HTP	Pitch/μm	T_{ce}/°C
A_0	0	737	741	4	7.04	0.473	66.2
A_1	1	687	707	20	7.07	0.441	64.3
A_2	2	661	698	37	7.09	0.422	62.8
A_3	3	594	634	40	7.25	0.383	60.4
A_4	4	518	568	50	7.92	0.332	54.8

[a]Added chiral monomer A6B. [b]Before UV irradiation. [c]After UV irradiation.

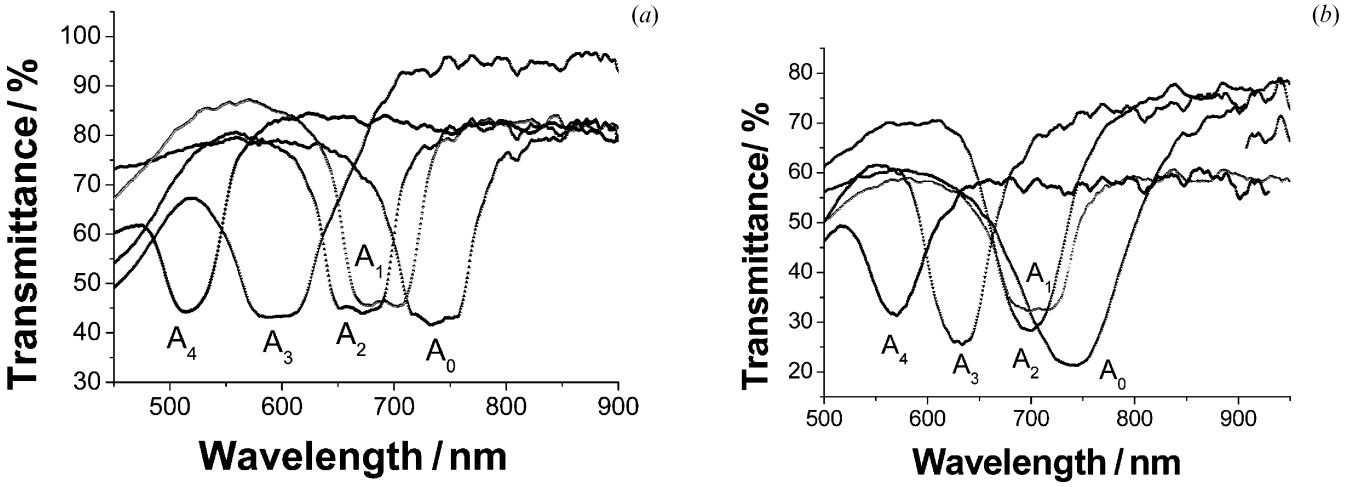

Figure 1. Effect of UV curing on the reflected band; (*a*) before and (*b*) after UV irradiation.

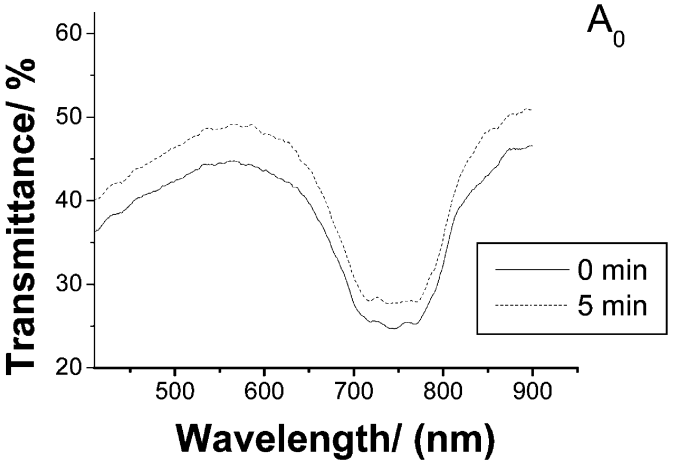

(*a*)

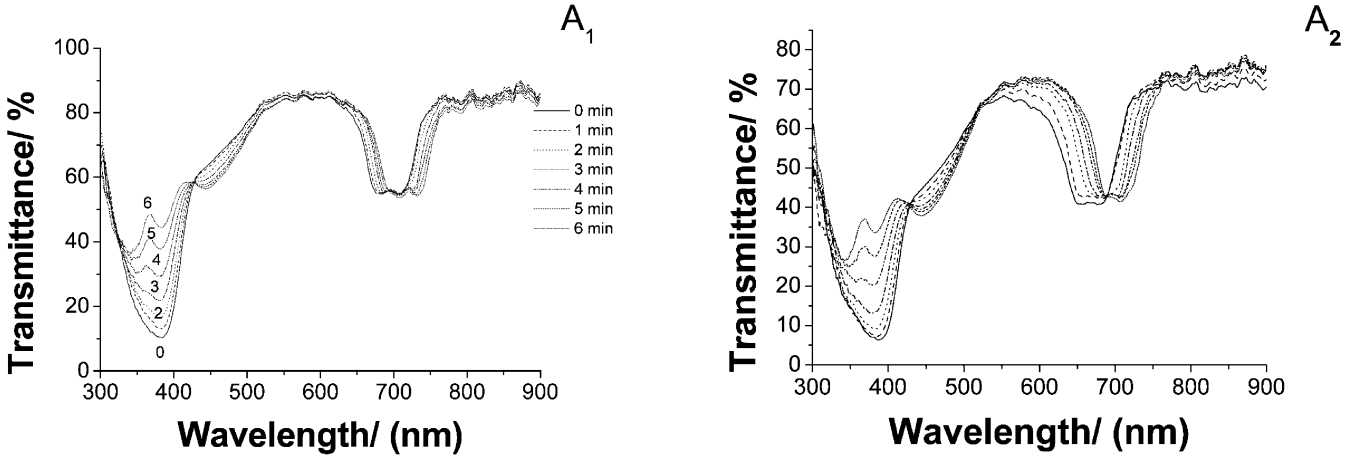

(*b*) (*c*)

Figure 2. Dependence of the cell transmittance on UV irradiation time: (*a*) A_0, (*b*) A_1 and (*c*) A_2.

Table 2. Effect of UV irradiation on optical properties of cells.

	λ_0/nm		
Cell[a]	Before[b]	After[c]	$\Delta\lambda_0$
A_0	741	741	0
A_1	690	724	34
A_2	661	707	46
A_3	600	670	70
A_4	520	642	122

[a]After polymerization. [b]Before UV irradiation. [c]After UV irradiation.

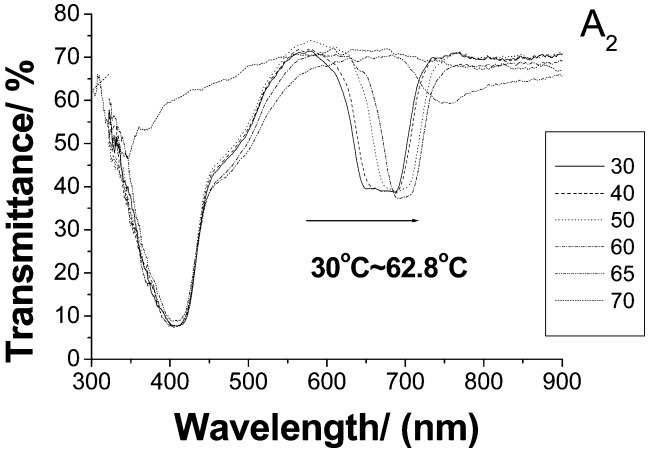

Figure 3. Effect of heating on the reflected band of cell A_2.

temperature on the reflected band of the cell; it was shifted to red on heating the cell. The cell was changed to the isotropic liquid phase on heating above the clearing point of 62.8°C; the reflected band then disappeared.

The textures of the prepared cholesteric liquid crystal cells were investigated by POM. Figure 4 shows the POM texture of the cells with various amounts of polymer matrix. Without a polymer matrix, as shown in figure 4 (*a*), many spots appeared in cell A_0. As can be seen in figures 4 (*b*) to 4 (*e*), the existence of a polymer matrix stabilizes the cholesteric liquid crystal molecules, leading to the formation of a spread network-like texture.

Figures 5 and 6 show the POM textures resulting from UV irradiation and thermal effects on cell A_3, respectively. Figures 5 and 2 show that UV irradiation may cause a photo-induced isomerization of azo molecules from the *trans*- to *cis*-form and disturb the liquid crystal alignment leading to the formation of black spots. Finally, an isotropic phase was obtained, which showed a black image under crossed polarizers. As shown in figures 3 and 6, increasing the temperature raises the molecular mobility and disturbs the alignment of the liquid crystal molecules. The growth of spots in the POM textures illustrates the increasing disturbance. As described in figure 3, above the clearing temperature, the liquid crystal changes to the isotropic phase and a black image appears, see figure 6.

Liquid crystal molecules are anisotropic and usually sensitive to the power voltage. Figure 7 shows the dependence of the transmittance of cell A_3 on the voltage. As can be seen in figure 7 (*a*), cell A_3 exhibited a clear appearance when 100 V was applied, and an unstable focal-conic with opaque appearance at zero voltage. Figure 7 (*b*) shows a dynamic recording of the cell transmittance with variation of the applied voltage.

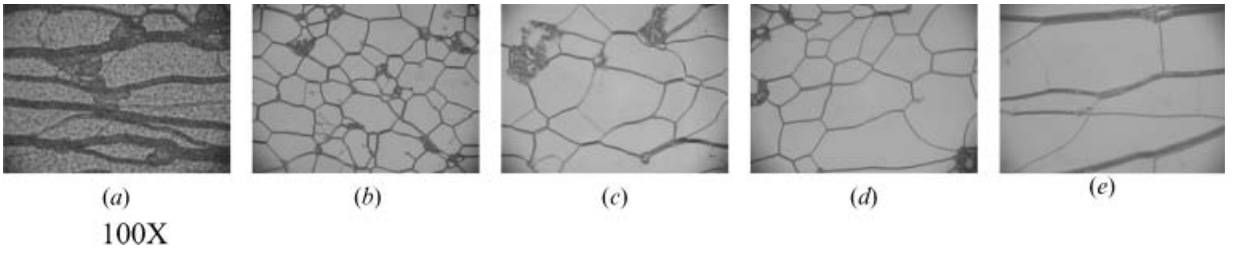

Figure 4. POM textures of (*a*) cell A_0 (*b*) cell A_1 (*c*) cell A_2 (*d*) cell A_3 (*e*) cell A_4.

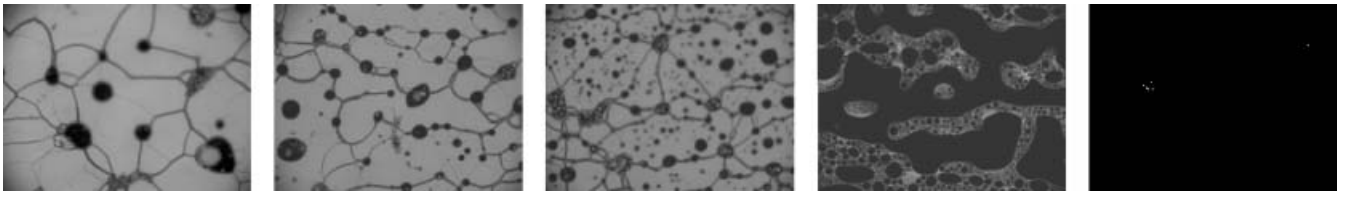

Figure 5. Effect of UV irradiation on POM textures of cell A_3. Irradition time increasing R.

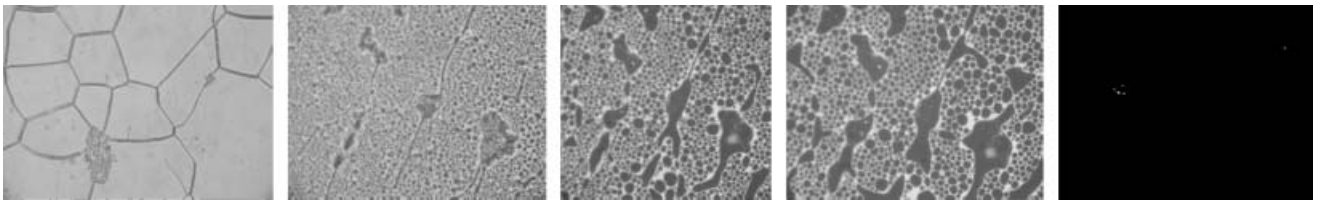

Figure 6. Temperature dependence on the textures of cell A_3. Temperature increasing R.

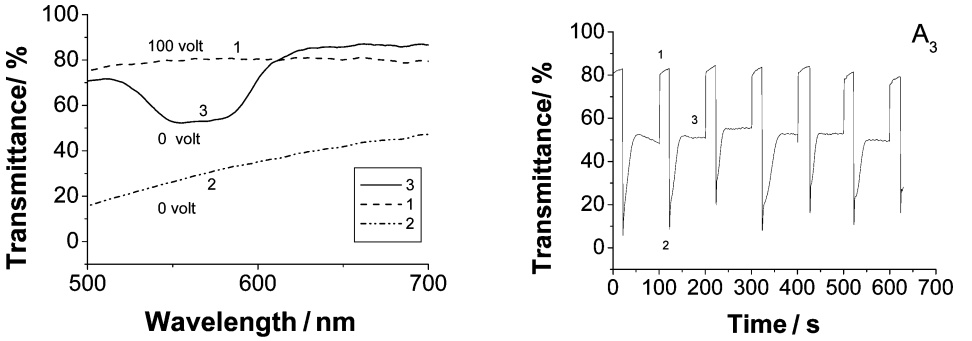

(*a*) (*b*)

Figure 7. (*a*) Dependence of transmittance of cell A_3 on voltage; (1) homeotropic, (2) focal conic, (3) planar. (*b*) Dynamic cell transmittance with variation of applied voltage.

Before the cell changed from the homeotropic to the planar state, it went through an unstable focal-conic transition state. The dependence of cell texture on applied voltage is summarized in figure 8. The texture of the liquid crystal changed with alteration of the alignment of the liquid crystal molecules due to the applied voltage. The cell was changed to a black appearance under POM, figure 8 (*d*), when 100 V was applied to the cell, and the liquid crystal molecules moved in to homeotropic alignment.

Schemes 2 (*a–c*) illustrate the operation of a PSCT liquid crystal cell. The cell comprises a pair of transparent substrates, a pair of transparent electrodes, and a polymer stabilized cholesteric liquid crystal medium located between the electrodes. A polymer network stabilizes the liquid crystal material. As shown in scheme 2 (*a*), in the voltage off-state the planar texture is stable and the helical axes of the cholesteric liquid crystal material are substantially perpendicular to the surface of the substrate on which natural or artificial light impinges. The planar texture selectively reflects incident light centred at the Bragg wavelength, $\lambda_0 = nP$, where n is the average index of refraction of the liquid crystal material and P is the pitch length of the helical structure of the liquid crystal material. The pitch P can be selectively varied by adding chiral agents which affect the pitch of the cholesteric liquid crystal material, and thus also the Bragg wavelength λ_0. As shown in scheme 2 (*b*), when a low voltage is applied between the electrodes the planar texture of the cholesteric liquid crystal material is transformed into a focal-conic texture, in which the helical axes of the liquid crystal are randomly aligned. In this state, the cell is substantially light transparent. If the applied

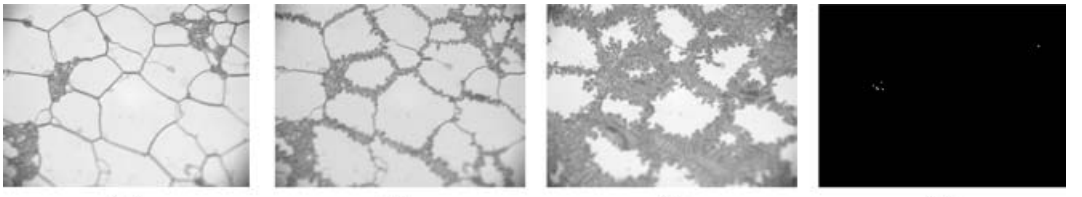

(*a*) (*b*) (*c*) (*d*)

100X

Figure 8. Dependence of applied voltage on A_3 cell; (*a*) no applied voltage, (*b–d*) voltage was increased gradually to 80 V.

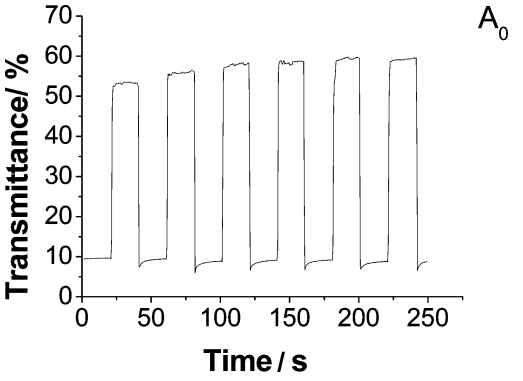

Figure 9. Dependence of cell transmittance on applied voltage (70 V).

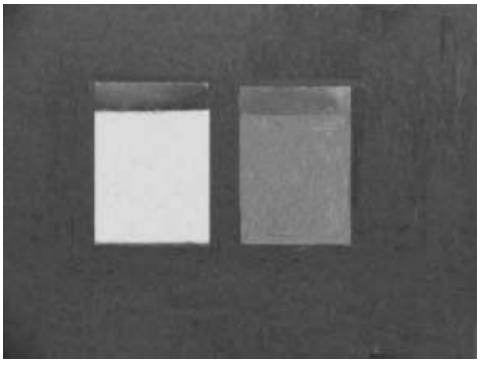

Figure 10. Real images of the reflected bands of the cells.

voltage is then removed, the focal-conic texture remains fixed due to the stabilizing effect of the polymer network. If a greater field is applied to the display, scheme 2 (*c*), the cholesteric liquid crystal material becomes completely aligned and completely transparent. In figure 7 (*a*), the cell transmittance indicates the variation of the liquid crystal texture due to applied voltages.

It has been reported that the response of a polymer stabilized cholesteric liquid crystal material to the release of the applied field is dependent on the rate of release of this field [28]. Quickly releasing this field causes the cholesteric liquid crystal material to relax back to the planar texture shown in scheme 2 (*a*). If the field is released more slowly, the cholesteric liquid crystal material will relax back to the focal-conic texture shown in scheme 2 (*b*). This bistable memory capability of polymer stabilized cholesteric texture LCDs can significantly reduce the power consumption of the displays in many applications, because the displays consume no power when viewed and needs only to be powered for short periods of time to change the displayed image. However, as shown in figure 7 (*b*), bistable states could not be seen in our experiments. The cell thickness in our system is 12 µm. Surface stabilization from the polymer matrixes on the substrates could not fix the focal-conic texture, even though the cell was released slowly from the applied field. The liquid crystal molecules returned to a planar texture in a few seconds.

Figure 9 shows the reliability and stability of the dependence of the transmittance on applied voltage; repeatable and stable ON/OFF optical behaviour was obtained. Figure 10 shows the real colour variation of cells such as those described in figure 1, where variation of the reflected band revealed different colours.

Figure 11 shows the reversible turbid and transparent changes corresponding to (*a*) OFF (30 V) and (*b*) ON (100 V) applied electric fields. A fabricated PSCT cell was set in front of a picture of liquid crystal texture. As shown in scheme 2 (*b*), in the case of the low electric field, the focal-conic structure is formed and causes the light scattering phenomena. When a higher electric field is applied, scheme 2 (*c*), the liquid crystal director reorients parallel to the direction of the applied field, and the PSCT cell becomes transparent. The results are consistent with those results shown in figure 7 (*a*).

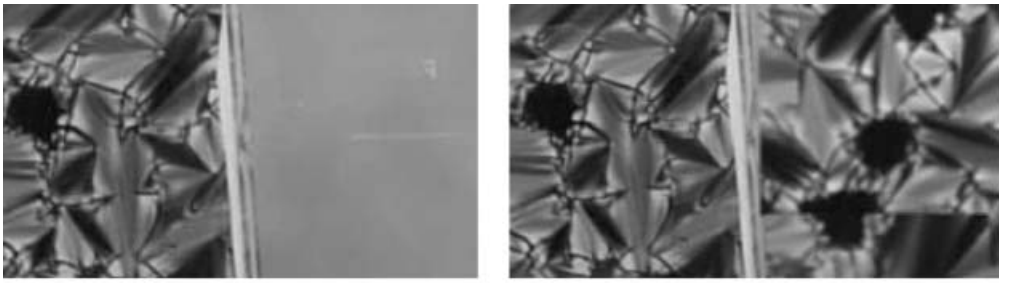

Figure 11. Reversible turbid and transparent changes corresponding to fields: (*a*) OFF (30 V), (*b*) ON (100 V).

4. Conclusion

Polymer stabilized cholesteric liquid crystal cells were fabricated using a host chiral nematic liquid crystal and functional monomer, and their optical behaviour was investigated. The effects of chiral dopants, heating, and UV irradiation on the cells were studied. Chirality and molecular interactions were found to affect the pitch of the cells, as well as the reflected bands. The planar texture of the PSCT cells was changed to focal-conic when a low voltage was applied. Due to the thick film gap, surface stabilization from the polymer matrixes on the substrates could not fix the focal-conic texture. When a high voltage was applied the director of the liquid crystal molecules was reoriented parallel to the applied field direction. Repeatable and stable ON/OFF optical behaviour and real images of the PSCT cells were obtained. Reversible turbid and transparent changes corresponding to OFF (30 V) and ON (100 V) applied electric fields were also achieved.

Acknowledgements

The authors would like to thank the National Science Council (NSC) of the Republic of China (Taiwan) for financial support of this research under Contract No. NSC 92-2216-E006-005.

References

[1] H. Kikuchi, T. Fujii, M. Kawakita, et al. *Appl. Opt.*, **43**, 132 (2004).
[2] A.Y.G. Fuh, C.R. Lee, K.T. Cheng. *Jpn. J. appl. Phys.*, **142**, 4406 (2003).
[3] L. Sannier, H.M. Siddiqi, U. Maschke, et al. *J. appl. polym. Sci.*, **92**, 2621 (2004).
[4] A.Y.G. Fuh, C.Y. Huang, M.S. Tsai, et al. *Jpn. J. appl. Phys.*, **35**, 630 (1996).
[5] K.Y. Yo, C.Y. Huang, G.C. Hsu, et al. *Jpn. J. appl. Phys.*, **142**, 3531 (2003).
[6] R. Barchini, J.G. Gordon, M.W. Hart. *Jpn. J. appl. Phys.*, **137**, 6662 (1998).
[7] H. Guillard, P. Sixou, L. Reboul, et al. *Polymer*, **42**, 9753 (2001).
[8] M.H. Lu. *J. appl. Phys.*, **81**, 1063 (1997).
[9] W.J. Zhang, J.P. Lin, T.S. Yu, et al. *Eur. polym. J.*, **39**, 1635 (2003).
[10] L. Sannier, H.M. Siddiqi, U. Maschke, et al. *J. appl. polym. Sci.*, **92**, 2621 (2004).
[11] A.Y.G. Fuh, C.Y. Huang, C.R. Sheu, et al. *Jpn. J. appl. Phys.*, **33**, L870 (1994).
[12] F. Vicentini, J.L. Cho, L.C. Chien. *Liq. Cryst.*, **24**, 483 (1998).
[13] R.M. Henry, R.A. Ramsey, S.C. Sharma. *J. polym. Sci. polym. Phys.*, **42**, 404 (2004).
[14] L.V. Natarajan, C.K. Shepherd, D.M. Brandelik, et al. *Chem. Mater.*, **15**, 477 (2003).
[15] D.S. Seo, J.H. Lee. *Jpn. J. Appl. Phys.*, **38**, L1432 (1999).
[16] T.J. Bunnning, L.V. Natarajan, V.P. Tondiglia. *Polymer*, **37**, 3147 (1996).
[17] R. Jakubiak, D. Brown, V.P. Tondiglia, et al. Abstr. Pap. Am. Chem. Soc., 226, 31-PMSE Part 2 (2003).
[18] H. Ren, S.T. Wu. *J. appl. Phys.*, **92**, 797 (2002).
[19] H. Guillard, P. Sixou, L. Reboul, et al. *Polymer*, **42**, 9753 (2001).
[20] T.C. Ko, Y.H. Fan, M.F. Shieh, et al. *Jpn. J. appl. Phys.*, **140**, 2255 (2001).
[21] J.H. Liu, F.R. Tsai, T.Y. Tsai. *Polym. adv. Technol.*, **11**, 228 (2000).
[22] J.H. Liu, H.Y. Wang. *J. appl. polym. Sci.*, **91**, 789 (2004).
[23] J.H. Liu, F.T. Wu. *J. polym. Res.*, **11**, 43 (2004).
[24] R.A.M. Hikmet. *J. Appl. Phys.*, **68**, 4406 (1990).
[25] J.H. Liu, F.T. Wu. *J. appl. polym. Sci.* (to be published) (2004).
[26] J.H. Liu, H.J. Hung, et al. *J. Appl. Polym. Sci.* (submitted) (2004).
[27] J.H. Liu, H.Y. Wang, C.H. Ho. *J. polym. Res.*, **10**, 13 (2003).
[28] G.P. Crawford, et al. In *Proceedings of the IS & T/SID*, 1995 Colour Imaging Conference: Color Science, Systems and Applications, 52 (1995).